46th Annual Review of Progress in Quantitative Nondestructive Evaluation QNDE2019
July 14-19, 2019, Portland, OR, USA

QNDE2019-6757

PIPELINE MAGNETIC SHIELD MODELING FOR DEFORMATION AND DISPLACEMENT DETECTION

Yu Zhang, Xinjing Huang*, Jian Li, Hao Feng
State Key Laboratory of Precision Measuring Technology and Instruments, Tianjin University, Tianjin, People's Republic of China

ABSTRACT

Pipeline magnetic shield factors are key parameters for magnetic inspections of pipeline trajectory, deformation, and displacement. This paper reveals the magnetic shielding model of long pipelines via simulation analyses based on the finite element simulations and experiments of the magnetic shielding of long pipelines. It is demonstrated that the radial and axial shielding factors of a finite pipe can be accurately calculated by the FEM; for a long pipeline consisting of many short sections, the averaged shielding factors over a couple of adjacent sections are equal to that of an ideal infinite pipeline, and the axial factor is always equal to 1.

Keywords: cylindrical magnetic shield, magnetic fields, pipeline orientation

1. INTRODUCTION

Steel pipelines are the most important infrastructure for transporting oil and natural gas. Security issues are one important aspect of pipeline operation management. Magnetic measurement of pipeline deformation and displacement is a novel and promising inspection method for pipeline integrity [1][2].Pipeline magnetic shield factorsare key parameters for pipeline magnetic inspections. First, it determines the calculation accuracy of the pipeline direction and trajectory by using the internal magnetic fields [3][4]. Second, the shielding factorof a pipelinecan be used to predict the internal magnetic fieldsunder normal conditions as important contrasts to those when abnormal deformation and displacement changes occuraccompanied with stress concentrationsconsidering the magneto-mechanical effects [5][6].

However, exact solutions for both axial and radial orientations of shield shells only exist for infinite cylinders or spheres. The magnetic fields inside a finite cylindrical shield, which is practical, realizable, and most widely used, can only be approximately solved [7-10]. One such approximation uses the ‘‘demagnetizing’’ factor of an ellipsoid with appropriate radii, where the cylinder is approximated by the ellipsoid [11][12]. This approximation is only valid for a limited range of geometric parameters.

The magnetic shielding of a long pipeline has not been modeled yet because it consists of many welded short sections, whose magnetic shielding effects are randomly distributed, relatively independent, and mutually influential. In one hand, field pipelines are very long, usually several or even tens of kilometers, and it is reasonable for them to be considered infinitely long. On the other hand, each section is of finite length and has various magnetic permeabilities and/or permeability distributions.These sections have unpredictable complicated original magnetizations at different parts, imprinted during molding and being changed by physical stresses while smithing and further treatment processes. Under the action of the hysteresis and magneto-mechanical effects, the traditional ideal magnetic shielding models are incapable of describing the magnetic fields inside the pipeline.

This work will answer two questions viaclassical shield model, finite element simulations, and experiments: (i) Whether the magnetic shielding of the pipeline complies with the ideal infinite model or the finite model; (ii) How to accurately calculate and obtain the shielding factors of the long pipelines.

2. FEM-BASEDANALYSES AND VERIFICATIONS

2.1 Classical shielding model

The magnetic shielding factors are defined as the ratio of the internal magnetic flux densityB_1 and the ambient magnetic flux density B_0:

$$\lambda_i = B_{1i} / B_{0i} \ , \qquad (1)$$

where$i$ = r or a, denoting radial or axial component. The infinite pipe model (IPM) asserts infinite pipes have no shielding effect in the axial direction, namely, λ_a= 1, and the radial shielding factor is as Eq.(2) [13]. An oil/gas/water pipeline can be assumed to be infinite relative to its diameter, so the cylindrical infinite cavity model can possibly characterize its shielding effectiveness, which needs numerically or experimentally verified.

$$\lambda_r = \frac{4\mu_r p}{(\mu_r^2+1)(p-1)+2\mu_r(p+1)} \approx \frac{4p}{\mu_r(p-1)+2(p+1)} \quad \text{when } \mu_r >> 1 \tag{2}$$

where $p = \frac{(R+d)^2}{R^2}$ and $R=D/2$.

2.2 Infinite pipelines simulated by torus pipes without ends

The simulation results above show that no matter how long a pipe is the shielding model cannot transit to an infinite one due to the magnetic charges at the ends. A field pipeline is very long and can be assumed infinite and without ends. Torus pipe has no ends and can be equivalent to an infinite pipeline when the curvature is small enough. The configurations of the torus simulation model are shown in **Fig.1(a)**. The larger the torus radius r is, the closer to a straight pipe the torus is. The magnetic fields in tori with different curvatures are calculated with the FEM by sweeping r, and the magnetic shielding factors are calculated by using Eq.(3). As show in **Fig.1(b)**, the shielding factors converge to the results of the IPM with the increase of r. The shielding factors converge to constant values when $r>r_0$=10m. The torus can be considered straight from a local perspective when $r>r_0$=10m and D=80mm.

$$\lambda_r = \frac{B_{1r}}{B_{0r}} = \frac{B_{1x}\cos\phi + B_{1y}\sin\phi}{B_{0x}\cos\phi + B_{0y}\sin\phi}$$
$$\lambda_a = \frac{B_{1a}}{B_{0a}} = \frac{-B_{1x}\sin\phi + B_{1y}\cos\phi}{-B_{0x}\sin\phi + B_{0y}\cos\phi} \tag{3}$$

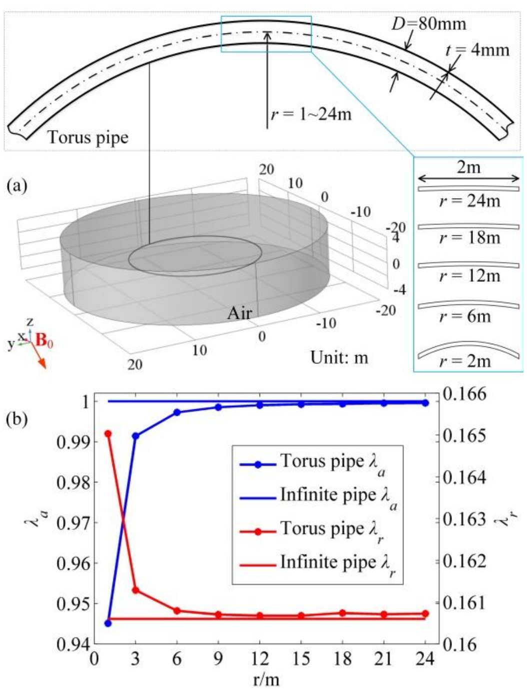

FIGURE 1: MAGNETIC SHIELDING FACTORS FOR TORUS PIPES TO SIMULATE INFINITE PIPELINES. (a) SIMULATION CONFIGURARIONS; (b) λ_a AND λ_r VS THE TORUS RADIUS r.

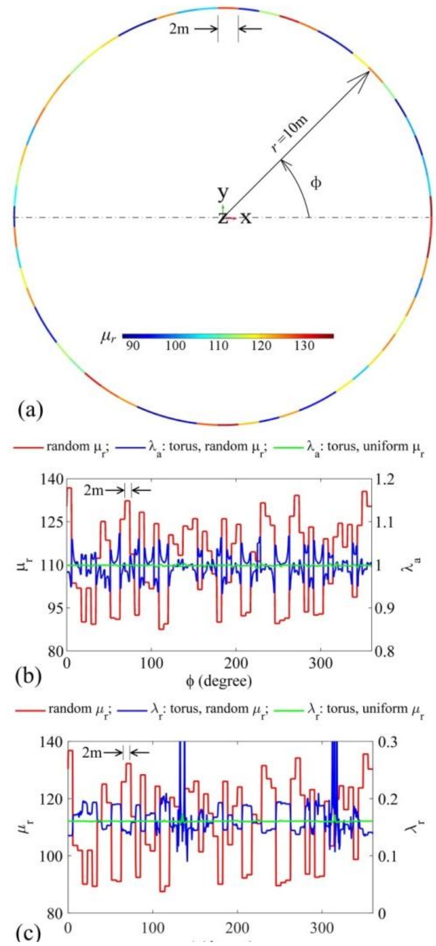

FIGURE 2: MAGNETIC SHIELDING FACTORS FOR A LARGE THIN TORUS PIPE WITH NON-UNIFORM μ_r DISTRIBUTIONS. (a) RANDOM μ_r DISTRIBUTIONS WITH AN AVERAGE OF 112; λ_a (b) AND λ_r (c) OF THE TORUS PIPE WITH RANDOM/UNIFORM μ_r.

The later experiments demonstrate the magnetic shielding factors of short pipes are randomly distributed, so the overall equivalent permeability μ_r of each section is also randomly distributed. Another torus with the permeability randomly distributed is employed to simulate a field pipeline consisting of a number of short pipes. The torus is with r=10m, D=80mm, and d=4mm, and the section length is 2m, as shown in **Fig.2(a)**. μ_r is randomly distributed among each section in the range of $(\bar{\mu}_r - \Delta\mu_r\ ,\ \bar{\mu}_r + \Delta\mu_r)$ with an average of $\bar{\mu}_r$. By taking $\bar{\mu}_r = 112$ and $\Delta\mu_r = 25$, the explicit values of μ_r are plotted as the red curves in **Fig.2(b)** and **(c)**. As a comparison, a torus of the same size with a uniform permeability μ_r=112 are also modeled and calculated. The results are shown in **Fig.2(b)** and **(c)**. The axial shielding factor λ_a varies inversely with the change of μ_r, and randomly fluctuates around the λ_a of the torus pipe with uniform permeability. The radial shielding factor has the same characterization. It can be concluded that the average shielding factors of a pipeline which consists of multiple sections are equal to that of an ideal infinite pipeline with the average permeability of those sections. The field pipeline shielding factors statistically comply with the IPM. Changing the values of $\bar{\mu}_r$ and $\Delta\mu_r$ does not change this conclusion.

Because of random original magnetizations and various permeability of each section, the magnetic fields inside pipelines are not uniform even for those adjacent sections in the same direction. However, as the direction of the pipeline changes slow, if the average magnetic components $\overline{B_{1i}}$ inside and the average shielding factors $\overline{\lambda_i}$ of these pipe sections are employed instead, then Eq.(1) can still strictly holds as follows $\overline{\lambda_i} = \overline{B_{1i}}/B_{0i}$, where i=r(radial) or a(axial), λ_a=1, and λ_r can be calculated by using Eq.(2) or the FEM. There is a clear and predictable mathematical relationship between the magnetic field inside the pipeline and the direction of the pipeline, which can be used to measure the pipeline orientation.

3. RESULTS AND DISCUSSION

In order to verify and refine the above results, we measured the magnetic fields inside steel pipes of different sizes and calculated the shielding factors. Magnetic measurements were carried out on a square in the open air with no disturbing magnetic sources around. The test environment and pipes are shown in **Fig. 3** (a) and (b). The measurements are accomplished by an anisotropic magneto-resistive magnetometer array. FPGA controller synchronously collects the magnetic signals of all the sensors via IIC bus and transmits them to the host computer through USB for saving and display. The magnetic field inside the pipe is not uniform. Therefore, in the later analyses, the average of the measuring points in the middle area, where the fields are more uniform, is used to calculate the shielding factors in order to reduce the calculation error.

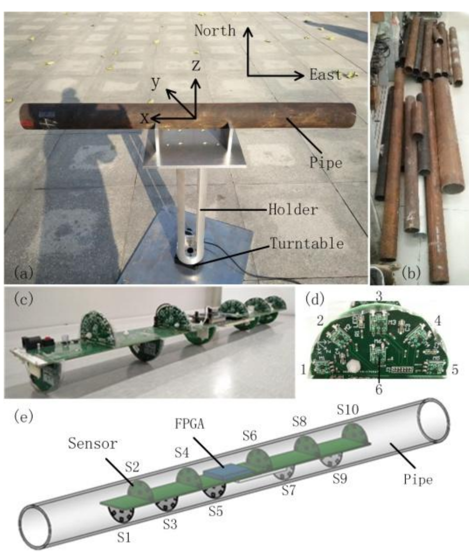

FIGURE 3: EXPERIMENTAL APPARATUS. (a) NON-MAGNETIC ROTATION PLATFORM; (b) TESTED PIPES; (c) AND (d) MAGNETIC SENSOR ARRAY; (e) SENSOR NUMBERINGS AND DISTRIBUTIONS.

The measured shielding factors of these pipes are random and less than 1. The shielding factors are different and disperse even if the pipe sizes are identical. The only reason is that the permeability significantly differs for different pipes due to the variety of the original magnetization during the production process. Therefore, the FEM simulations for all these pipes are carried out to sweep the permeability and search the best-matched permeability value. The calculated factor vs permeability curves and the measurement points are plotted together, as shown in **Fig.4**.Those discrete points can perfectly overlap those curves. There is always one value for the permeability that can be found to have the measured factor exactly equal to the FEM calculated factor. The simulation results are also confirmed to be correct.

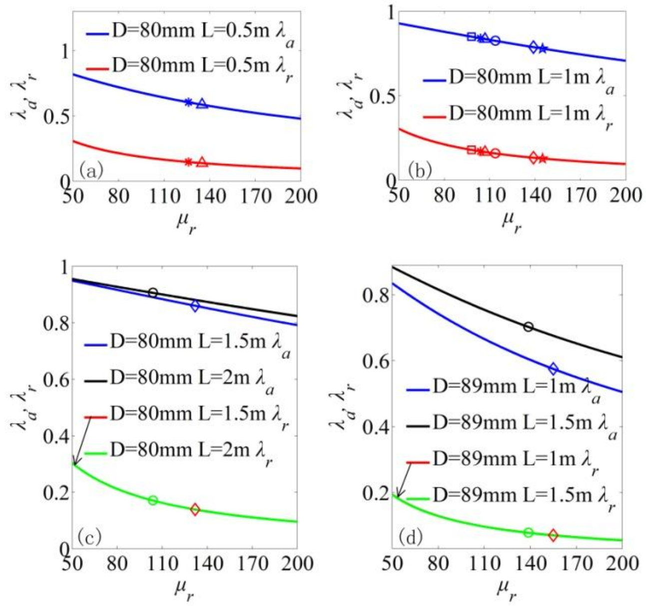

FIGURE 3: SWEEP μ_r TO MAKE THE MEASURED λ_a AND λ_{rv}EQUAL TO THAT OBTAINED VIA FEM BASED SIMULATIONS.

4. CONCLUSION

This work reveals the magnetic shielding model of long pipelines via simulation analyses based on the FEM and experimental verifications of the magnetic shielding of field long pipelines aiming at pipeline trajectory, deformation, and displacement detections. The radial shielding factor λ_r of a finite pipe can be correctly and accurately calculated by both the FEM and the IPM. The average shielding factors of a pipeline which contains multiple sections with different permeabilities are equal to that of an ideal infinite pipeline with the average permeability of those sections. The field pipeline shielding factors statistically comply with the IPM.

ACKNOWLEDGEMENTS

This work was supported by National Natural Science Foundation of China (No. 51604192, 61773283 and 61473205).

REFERENCES

[1] Liu Bin, He Luyao, Ma Zeyu, Zhang Hai, Sfarra Stefano, Fernandes Henrique, Perilli Stefano. Study on internal stress damage detection in long-distance oil and gas pipelines via weak magnetic method. Source: ISA Transactions, 2019,

Article in Press,
https://linkinghub.elsevier.com/retrieve/pii/S0019057818305044

[2] Huang Xinjing, Chen Guanren, Zhang Yu, Li Jian, Xu Tianshu, Chen Shili. Inversion of Magnetic Fields inside Pipelines: Modeling, Validations, and Applications. Structural Health Monitoring-An international journal, 2018, 17(1): 80-90.

[3] Xinjing Huang, Shili Chen, Shixu Guo, Tianshu Xu, Qianli Ma, ShijiuJin, Gregory S. Chirikjian. A 3D localization approach for subsea pipelines using a spherical detector. IEEE Sensors Journal, 2017,17(6): 1828-1836.

[4] Zhao Wei, Huang Xinjing, Chen Shili, Zeng Zhoumo, JinShijiu. A detection system for pipeline direction based on shielded geomagnetic field, International Journal of Pressure Vessels and Piping, 2014, 113:10-14.

[5] Jiles D C. Theory of the magnetomechanical effect. Journal of Physics D Applied Physics, 1998, 28(8): 1537-1546.

[6] Zeng Zhoumo, Zhao Chengwu, Huang Xinjing, Li Jian, Chen Shili. Non-invasive pressure measurement based on magneto-mechanical effects, Measurement Science and Technology, 2018, 29(9): 095106-8.

[7] Sumner T J, Pendlebury J M, Smith K F. Convectional magnetic shielding. Journal of Physics D Applied Physics, 1987, 20(9):1095-1101.

[8] Mager A. Magnetic shields. IEEE Transactions on Magnetics, 1969, 6(1):67-75.

[9] Azizi D, Heydari H, Gholami A. Analysis of the shielding effectiveness of several magnetic shields. World Academy of Science, Engineering and Technology, 2010, 71:151–155.

[10] Malkowski S, Adhikari R Y, Boissevain J, et al. Overlap Technique for End-Cap Seals on Cylindrical Magnetic Shields. IEEE Transactions on Magnetics, 2013, 49(1):651-653.

[11] Mager A. Magnetic Shielding Efficiencies of Cylindrical Shells with Axis Parallel to the Field. Journal of Applied Physics, 1968, 39(3):1914-1914.

[12] Yeqing Hu, Chunsheng Lin, Jianjun Zhou. The Calculation of Magneto-static Shielding Effectiveness of Limited Length Cavity Cylinder Based on the Spheroid Model. Marine Electric & Electronic Technology, 2011,31(8):45-47, 55.

[13] Hongmin Lu, Menglin Xue, Junmei Fu. Analysis of magneto static shielding effectiveness of the infinite cavity cylinder with magnetic material. Jounal of Xidian University, 1999, 26(1): 80-83.